CLICdp-Draft-2016-003
18 January 2016

Precision Higgs boson measurement at CLIC

Mila Pandurović[1)]*

On behalf of the CLICdp collaboration

* *Vinca Institute of Nuclear Sciences, Mihajla Petrovica Alasa 12-14. Belgrade, Serbia*

Abstract

The design of the next generation collider in high energy physics will primarily focus on the possibility to achieve high precision of the measurements of interest. The necessary precision limits are set, in the first place, by the measurement of the Higgs boson but also by measurements that are sensitive to signs of New Physics. The Compact Linear Collider (CLIC) is an attractive option for a future multi-TeV linear electron-positron collider, with the potential to cover a rich physics program with high precision. In this lecture the CLIC accelerator, detector and backgrounds will be presented with emphesis on the capabilities of CLIC for precision Higgs physics.

Talk presented at The XIII-th International School-Conference, The Actual Problems of Microworld PhysicsGomel, Belarus, July 27 August 7, 2015
This work was carried out in the framework of the CLICdp collaboration

[1]milap@vinca.rs

1 Introduction

The particle that completed the Standard model (SM) picture, the Higgs boson, was discovered at the Large Hadron Collier (LHC) in 2012 [1][2]. Besides the measurement of the Higgs boson mass, measurements of other Higgs boson properties, like its couplings to the SM particles, require high precision in order to be sensitive to eventual signs of New Physics, as well as to understand the structure of the Higgs sector. The LHC, being the discovery machine, was designed to reach extremely high center-of-mass energy of 14 TeV at the ultimate stage of operation. Due to the composite nature of colliding particles, the actual collision occurs at the parton level. The effective center-of-mass energy available in the parton-parton collision is $\sqrt{s} \approx 3$TeV. Also, the initial state of colliding partons is not known, and it is determined statistically from the final state. Besides, the presence of high level of QCD background and multiple pile-up events restrict the precision of all measurements. On the other hand at the lepton colliders the colliding particles, electrons and positrons, are fundamental objects. Therefore collisions have a well-known initial state and low level of background. Furthermore all of the center-of-mass energy is available for the collision. These properties make the lepton colliders suitable candidates to be the precision machines.

1.1 CLIC accelerator

The particle acceleration at CLIC is based on a new, 'two-beam' acceleration technique. Two separate beam pipes, running in the parallel to each other, are carrying two beams: the drive beam and the main beam. The drive beam is carrying power for the acceleration, with frequency of 12 GHz, high current (100 A) and low energy of (2.4 GeV -240 MeV). This power is extracted from the drive beam and converted in radio-frequent power in PETS (Power Extraction and Transfer Structures). PETS are positioned along the drive beam and paired-up with the accelerating structures which are placed along the main beam (Figure 1) [3].

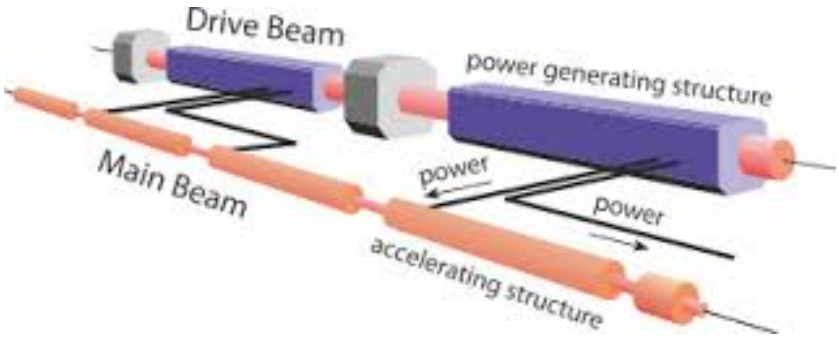

Figure 1: Two beam scheme: The beam power in the drive beam is converted to RF power in Power Extraction and Transfer Structures, and injected into accelerating structures in the main beam.

The energy extracted in the PETS is injected into accelerating structures and used to achieve the high energy (up to 1.5 TeV) in the main beam. The CLIC accelerating gradient is foreseen to be 100 MV/m.

The particles in the main beam are organized into bunches. The bunch population is $3.7 \cdot 10^9$ particles. Further, the bunches are organized into bunch trains of 312 bunches, with the bunch separation of 0.5 ns. Bunch trains are released with f_{rep}=50 Hz repetition rate. The two-beam acceleration scheme is one of the subjects of the study of the CTF3 test facility at CERN.

1.2 CLIC energy staged design

The energy staged design of the CLIC collider has been optimized to maximize the physics potential of the machine and provide an early start of physics. Three distinct stages were chosen, in the way to adapt

to the known physics and to eventual discoveries at the LHC.
Current studies foresee three stages, $\sqrt{s}$ =380 GeV, 1.4 TeV and 3 TeV. This would yield the collider overall length of 11.4 km, 27.2 km, and final extension to a length of 48.3 km, respectively, based on an accelerating gradient of 100 MV/m. The staging design is based on the foreseen physics program. The first stage of running, $\sqrt{s}$ =380 GeV, is devoted to the Standard model Higgs studies and exploration of the top physics, including $t\bar{t}$ threshold scan. The second stage, $\sqrt{s}$ =1.4 TeV, is chosen as it is sensitive to many of the Beyond Standard Model (BSM) models. Also the high statistics of the dominant WW-fusion Higgs production channel at this energy stage, gives access to rare Higgs processes, as well as to the Higgs self-coupling and quartic Higgs coupling. The final stage, $\sqrt{s}$ =3.0 TeV, improves the precision obtained at previous energy stages in both Higgs and BSM physics, and adds additional discovery potential.

1.3 CLIC experimental environment

One of the most important parameters of any collider experiment is its luminosity. At a linear e^+e^- collider the increase in luminosity is achieved by the optimisation of the beam parameters. The focusing of the beam, on the other hand, is limited by the energy loss by *beamstrahlung* caused by the electromagnetic interaction of the opposite beams.

1.3.1 Luminosity

The instantaneous luminosity is given by:

$$\mathscr{L} = \frac{n_b N^2 f_{rep}}{4\pi\sigma_x\sigma_y} \tag{1}$$

where σ_x, σ_y are transverse bunch sizes, N is the bunch population and n_b is the number of bunches in a bunch train. The increase in the luminosity at linear colliders is achieved by the using high bunch population, $\mathscr{O}(10^9)$, and small beam sizes.

1.3.2 Beam-induced background

The high bunch population and small bunch size results in a strong electric field of a bunch. This is causing the particles in the colliding bunches to accelerate towards the bunch center, subsequently radiating photons. The emission of this radiation, *beamstrahlung*, has a consequence that it degrades the luminosity spectrum. Figure 2 shows the luminosity spectrum for the 3 TeV CLIC [4]. The effect is most pronounced at the highest energy stage, where around 35% of events preserve the nominal of center-of-mass energy within the less then a percent energy loss.

The energy loss by beamstrahlung is proportional to:

$$\delta E \propto \frac{N^2}{(\sigma_x+\sigma_y)\sigma_z} \tag{2}$$

The maximal length of the bunch is limited by the Hourglass effect [5], thus in order to maximize the luminosity and minimize beamstrahlung energy loss, the flat beams, with the $\sigma_x \gg \sigma_y$ are chosen. For the final, 3 TeV energy stage the parameters foreseen are σ_x=45 nm, σ_y=1 nm.

The beamstrahlung photons can convert into electron positron pairs, or interact and produce hadrons in the final state. Such hadrons deposit 20 TeV of energy per bunch train in the central calorimeters. In addition, beamstrahlung is causing radiation damage to the very forward calorimeters.

Besides, the $\gamma\gamma \rightarrow$ hadrons background influences the event reconstruction, by the central tracker especially at the highest energy stage, where there is an average of 3.2 events per bunch crossing. This type of background is rejected using momentum and timing cuts, which drives challenging requirements on detector timing capabilities.

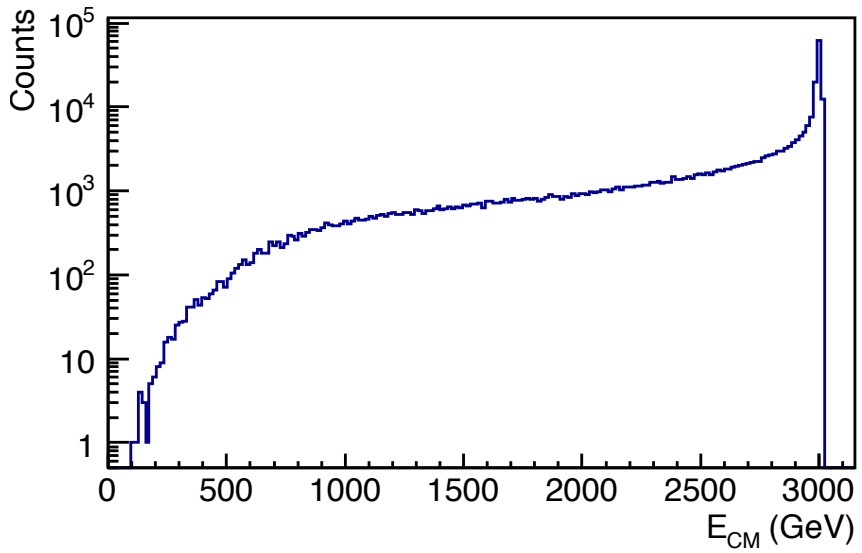

Figure 2: CLIC luminosity spectrum as a function of the effective center-of-mass energy.

1.4 CLIC detector

The recent CLIC detector concept has emerged from two detector concepts parallel developed, which were based on ILC detector models, CLIC_ILD [6], and CLIC_SiD [7]. The difference between the two models are in the tracking system, where the CLIC_ILD foresees a gaseous tracking (TPC), whereas CLIC_SiD uses a silicon tracker. All other detector systems are similar. These detectors were adapted to the CLIC beam and background conditions, which are different than ILC primarily due to the higher center-of-mass energies and beam structure.

The performance of each sub-detector system is driven from the physics requirements. In the first place, precision measurement of the momentum resolution of a track ($\frac{\sigma_{p_t}}{p_t^2}$) is required for the recoil mass measurement of the Higgs boson in the Higgsstrahlung process [3]. The impact parameter resolution is necessary for heavy flavor separation (bottom/charm), and to exploit the most probable Higgs decay channel, H $\rightarrow b\bar{b}$. The required impact parameter resolution in the transverse plane is $\sigma_{r\phi} = 5 \oplus \frac{15}{p \cdot sin^{3/2}(\theta)} [\mu m]$ [3]. Vertexing is performed with highly granulated, light-weight silicon pixel detector. Separation of the electroweak bosons requires good jet energy resolution in the calorimeters, which for the jet energies above 100 GeV is $\frac{\sigma_E}{E} < 3.5$ %.

These detectors are comprised in a strong solenoid field of 4-5 T. A muon system, implemented as an instrumented return yoke, surrounds the whole detector. Special calorimeters for luminosity measurement and beamstrahlung monitoring are foreseen in the very forward region, down to 1.5 deg, providing additional hermeticity of the detector, which is necessary for the missing energy signature measurements in many BSM processes.

2 Higgs physics at CLIC

Measurement of properties of the Higgs boson will be a priority for CLIC. In order to estimate the physics potential of CLIC in terms of precision Higgs measurements, a comprehensive list of Higgs physics benchmark studies is currently being carried out [8]. The most important measurements are those of Higgs mass and couplings of Higgs to the SM particles, including Higgs self-coupling. The

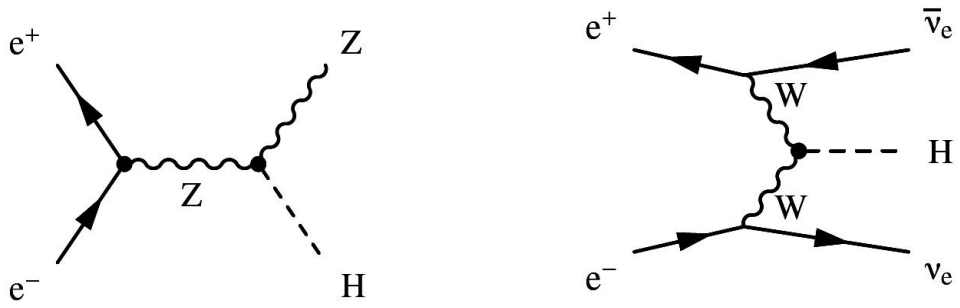

Figure 3: Feynman diagrams of the highest cross section Higgs production processes at CLIC; Higgsstrahlung (left), WW-fusion (right).

$\sqrt{s}$	380 GeV	1.4 TeV	3 TeV
	500 fb^{-1}	1.5 ab^{-1}	2 ab^{-1}
# HZ events	68,000	20,000	11,000
# WW-fusion events	17,000	370,000	830,000
# ZZ-fusion events	3,700	37,000	84,000

Table 1: Number of Higgs events expected for the leading-order Higgs production processes for m_H=126 GeV, including initial state radiation and CLIC beam spectrum, for unpolarized beams.

high precision measurement of the Higgs boson couplings would be a test of the SM, which predicts a strict linearity of the couplings to the corresponding masses. Any deviation from the predicted SM values would be a sign of BSM physics [9].

2.1 Higgs Production at Linear Colliders

Different center-of-mass energies at CLIC give rise to different Higgs production channels. At the lowest energy stage $\sqrt{s}$=380 GeV, the leading Higgs production channel is the s-channel Higgsstrahlung process (HZ), where the Higgs boson is radiated off a Z boson. The corresponding Feynman diagram is given in Figure 3. This energy stage is in the first place dedicated to the model independent measurement of the total HZ cross-section and consequently to the absolute Higgs to Z coupling. Also at this stage the available statistics allows the determination of the cross-section of most of the Higgs decays, with the lightest accessible Higgs decay being the one to $c\bar{c}$. Besides, this energy stage allows the model independent measurement of the Higgs boson mass.

At higher energy stages, Higgs production is accessed predominantly by the t-channel WW-fusion, Figure 3 (right), where the cross-section rises logarithmically with energy. The available statistics allows more precise measurements of the Higgs couplings to be performed.
The distribution of the cross-sections for the various Higgs production channels is given in Figure 4 (left), for unpolarized beams.

Table 1. lists the number of Higgs events of the most relevant production processes expected in the studied CLIC staging scenario.

The cross-sections can be enhanced using polarised beams. For P_{e^-}=-80 % electron beam polarisation considered for CLIC, the listed numbers increase by 12% for ZH and ZZ-fusion events and 80% for WW-fusion production mechanisms.

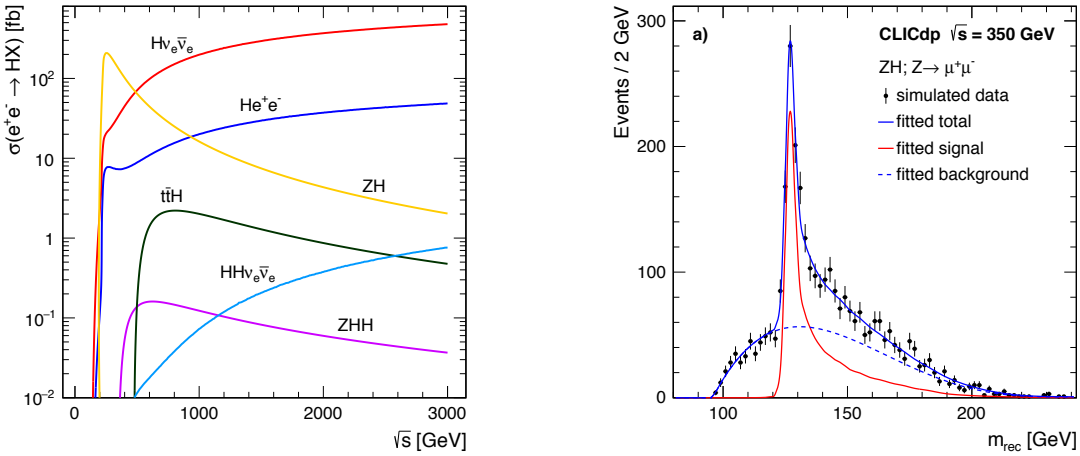

Figure 4: Left: The cross sections for the main Higgs production processes, as a function of center-of-mass energy, at an e^+e^- collider. Right: recoil mass distribution of muon pairs from Z decay at 380 GeV center-of-mass energy scaled to an integrated luminosity of 500 fb^{-1} .

2.2 Model independent Higgs boson measurements at linear collider

A unique feature of lepton colliders is a model independent Higgs recoil mass analysis in the Higgsstrahlung process, Figure 4 (right), which enables the measurement of the Higgs boson mass and total cross-section of the Higgsstrahlung process to be determined independently of the Higgs decay mode. The total HZ cross-section is proportional to the absolute coupling of the Z to Higgs boson and it is the starting point of the determination of all other absolute Higgs couplings.

The Higgsstrahlung process is identified by the pair of leptons (electrons or muons) with the invariant mass consistent with the Z mass and the recoil mass (m_{rec}) consistent with the mass of the Higgs boson. The distribution of the recoil mass is constructed using only the properties of the lepton pair, invariant mass (m_Z) and energy (E_Z):

$$m^2_{rec} = s + m^2_Z - 2E_Z\sqrt{s} \tag{3}$$

The distribution of the recoil mass, constructed for $\sqrt{s}$=380 GeV, Figure 4 (right), features a clear peak at the Higgs mass. The high energy tail is due to emission of beamstrahlung and initial state radiation.

In the analysis of the $Z \to \mu^+\mu^-$ decay, the Higgs mass is determined with an absolute statistical precision of 120 MeV. The relative statistical error of the total cross-section of the Higgsstrahlung process $\Delta(\sigma_{HZ})\ /(\sigma_{HZ})$ is determined by counting the number of events in the peak. For the combined muonic and electronic Z-decays $\Delta(\sigma_{HZ})\ /(\sigma_{HZ}) \approx 4\%$, with the resulting absolute coupling of Higgs to Z boson, $g^2_{HZZ} \approx 2\%$ [8].

The relative statistical error of the absolute Higgs to Z coupling, together with the total Higgs decay width, Γ_H, limits the precision of all other absolute couplings. The leptonic Z-decays give a clear signature of Higgsstrahlung events so the selection efficiency is independent of the Higgs decay mode. On the other hand it is limited by the low Z branching fraction of 3%. It has been shown that the hadronic Z decay channel, which has a high BR(Z$\to qq \approx 69\%$) can also be used, even though the hadronic Z reconstruction depends on the Higgs decay mode. It has been shown that careful selection criteria can be chosen, to ensure near model independence [10]. The clearest separation between signal and background is obtained from m_{qq} and the recoil mass m_{rec}, as shown in Figure 5. The signal is clearly peaked at $m_{qq} \sim m_Z$ and $m_{rec} \sim m_H$.

By combining the hadronic with leptonic channel the relative statistical error is improved to 0.8%.

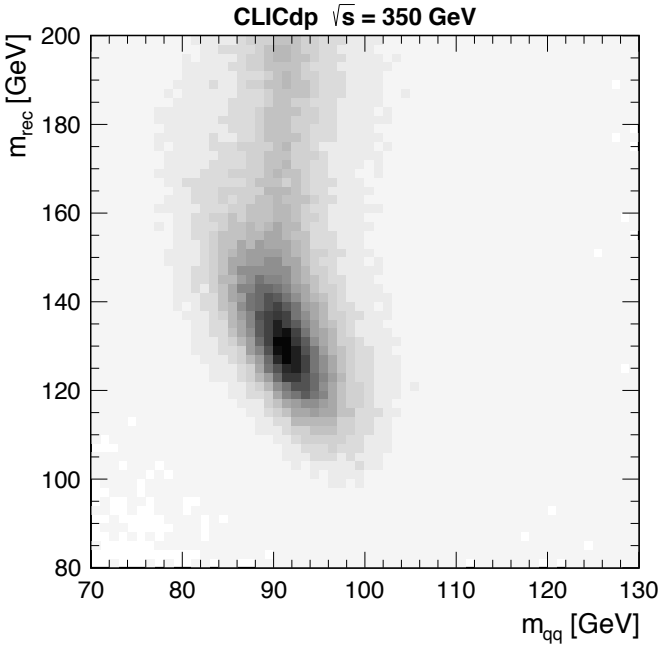

Figure 5: Reconstructed di-jet invariant mass versus reconstructed recoil mass distributions for selected ZH → qqX events at 350 GeV, given for signal events [10].

The total Higgs decay width, Γ_H, is obtained through the WW-fusion Higgs production channel with the consequent Higgs decay to a W pair, H→WW*, once g_{HWW} is known:

$$\sigma(e^+e^- \to H\nu_e\bar{\nu}_e) \times (H \to WW^*) \propto \frac{g^4_{HWW}}{\Gamma_H}. \tag{4}$$

Γ_H can be used to determine the absolute value of all other measured couplings.

2.3 The measurements of cross-sections of specific Higgs decays

The measurement of absolute couplings of the Higgs to the Z boson can be used to obtain absolute couplings of Higgs to other SM particles using measurements of partial cross-sections of type ($e^+e^- \to$ HZ,WW-fusion) × BR(H → $x\bar{x}$). This cross-section is proportional to the Higgs coupling to one of the vector bosons, depending on the production channel, g^2_{HZZ} for Higgsstrahlung or g^2_{HWW} for WW-fusion and to g^2_{Hxx} through the decay channel (H → $x\bar{x}$). All three energy stages are used to extract g^2_{Hxx} and Γ_H through $\frac{g^2_{HZZ} \cdot g^2_{Hxx}}{\Gamma_H}$, in a model independent way.

The first stage of CLIC operation, with the Higgsstrahlung as the leading Higgs production channel, enables the clean measurements of the branching fractions of the Higgs decays into the b and c quarks, τ, WW* and gluons using the reconstruction of the recoiling Z boson and the explicit reconstruction of the Higgs boson. For these measurements precise flavor tagging for the separation of b and c jets is crucial, as well as the excellent particle flow performance for the efficient identification of τ leptons and for the reconstruction of hadronic W decays. The branching ratio of H→gg can not be directly transformed to a coupling, but provides model-dependent sensitivity to the coupling to the top quark through loop contributions, since in the SM the coupling of the Higgs to the gluon is realized through a heavy quark loop. The Higgsstrahlung process cross-section can be increased by using the polarization P_{e^-}=-80% up to 12% [8].

At the higher energy stages the leading Higgs production channel is WW-fusion. The cross-section of this production process can be increased up to 80% with the maximal polarization P_{e^-}=-80%.The

abundant statistic is used to improve the precision of the coupling measurements obtained at the first energy stage. Also, the higher energy stages give access to the low cross-section processes, also offering a possibility to directly measure the coupling of the Higgs to the top quark using $e^+e^- \to t\bar{t}H$ process, which is sensitive to the top-Yukawa coupling. This process can be studied using the most favorable Higgs decay, $H \to b\bar{b}$, along with semileptonic and hadronic W decays. This complex final state, with 6 to 8 jets including four b-jets, is an excellent detector benchmark process, testing jet reconstruction, flavor tagging, lepton identification, and reconstruction of missing energy. The combined precision is $\Delta\sigma(t\bar{t}H) \,/\, \sigma(t\bar{t}H) = 8.1\%$ resulting in a precision on the top Yukawa coupling of 4.3%.

The measurement of the trilinear self-coupling provides direct experimental access to the shape of the Higgs potential. The $e^+e^- \to HH\nu_e\bar{\nu}_e$ process is available for measuring the trilinear Higgs self-coupling, with the cross-section rising with the center of mass energy. The study of this coupling using the most common Higgs decay mode $HH \to b\bar{b}b\bar{b}$ decay as the signal, achieves a precision on the Higgs trilinear self-coupling of 32% at $\sqrt{s}$ = 1.4 TeV and 16% at 3 TeV [8]. Using beam polarisation, this precision further improves to 24% and 12%, respectively.

The measurement of the quartic coupling g_{HHWW} are also possible at higher energy stages. The simulation studies have shown that the quartic coupling, using the $HH \to b\bar{b}b\bar{b}$ can be measured with a statistical uncertainty of 7% at $\sqrt{s}$ = 1.4 TeV and 3% at 3 TeV, including P_{e^-}=80% polarisation. These results could be improved by adding analyses for other Higgs decay channels such as $HH \to b\bar{b}WW^*$. The analysis of these Higgs decay channels represents a challenge for the forward jet reconstruction.

Also the sufficiently high statistics allows for the Higgs coupling measurement to the lightest SM particles, as in the Higgs decay to a pair of muons. This decay has extremely low BR of the order of 10^{-4}. The statistical precision of $BR(H \to \mu\mu) \times$ is 29% at the 1.4 TeV CLIC, and 16% at the highest energy stage 3 TeV.

The indirect couplings of Higgs to γ can also be accessed at higher energy stages. In the SM, this decay is induced via loop diagrams, dominated by heavy charged particles, mostly W bosons and t quarks. This measurement is highly sensitive to BSM physic proceses, which modify the effective $H \to \gamma\gamma$ branching ratio. It has been shown that the statistical uncertainty of 15% can be obtained at the 1.4 TeV energy stage. Simulation studies of the $H \to \gamma Z$ decay channel including both hadronic and leptonic (e,μ) Z decays reach a combined precision of the Higgs production cross-section times branching ratio of 42% at 1.4 TeV [11].

2.4 Combined Higgs Fit

The best result of the Higgs couplings and decay width measurement is obtained by a simultaneous model-independent fit performed using the results of all three energy stages. The starting point of this fit is the model-independent measurement of the couplings of Higgs to Z bozon g_{HZZ}. The free parameters of the fit are the uncertainties of the couplings as well as the total Higgs decay width. The relative statistical precision of the measurement of Higgs couplings to the SM particles is shown in Figure 6 (left). It has been shown that the relative statistical uncertainties can reach the percent level. The Higgs width is extracted with 3.5 % precision.

Better results can be obtained by using the fit which presumes that the total Higgs decay width is constrained by the Standard model, that is, that there are no unknown decays. The fit is performed in the same manner as at the LHC experiments. The free parameters of the fit are relative partial widths of the Higgs decays with respect to corresponding SM values. The uncertainty of the total Higgs decay width does not enter the fit, but is calculated using the uncertainties of the partial widths obtained in the fit. The relative statistical uncertainty obtained by this method improves and reaches the subpercent level for the most of the measurements except the rare Higgs decays, like $H \to \gamma\gamma$ or $H \to \mu\mu$. However, the results of this fit are model dependent. The results of the model-dependent fit are shown in Figure 6 (right).

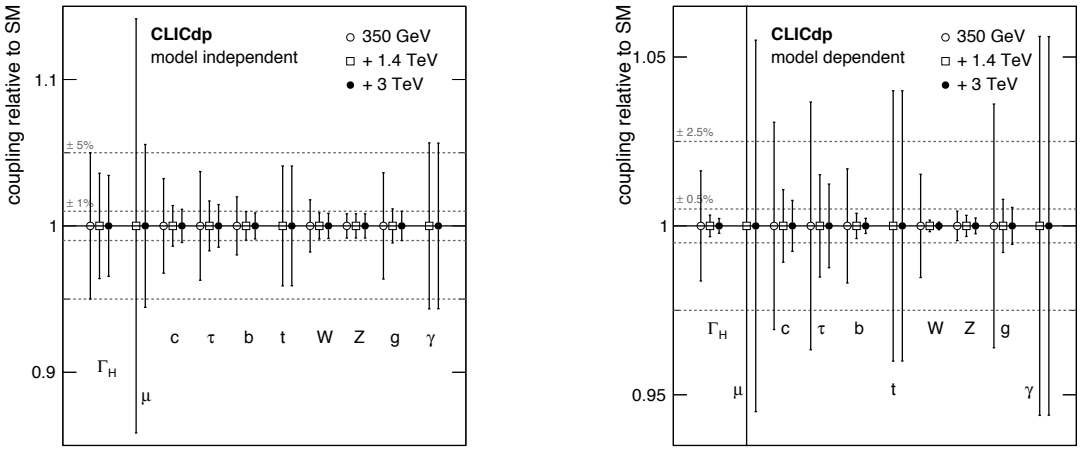

Figure 6: Illustration of the achievable precision on the Higgs couplings and decay width, obtained in a fit using three successive CLIC energy stages. Left: Model-independent fit. right: model-dependent fit. The impact of electron polarization of -80 % at $\sqrt{s}$= 1.4TeV and 3 TeV energy stages are included as a scale factor.

2.5 Conclusion

In this lecture, the motivation for a e^+e^- collider as a next generation facility in high energy physics is given. One of the possible options is the Compact linear collider CLIC, operating at three centre-of-mass energy stages, 380 GeV, 1.4 TeV and 3.0 TeV. The principle of CLIC particle acceleration, the detector concepts and working conditions have been presented in some detail. The focus of the lecture was put on the capability of CLIC for a comprehensive precision Higgs physics program.

The initial stage of operation, 380 GeV, allows the study of Higgs production from both the HZ and the WW-fusion process. These data would yield precise model-independent measurements of the Higgs-boson couplings. The obtained statistical precision of the absoulte Higgs to Z boson coupling is g_{HZZ} = 0.8%, and the total Higgs width is measured with the statistical precision of 5.0 %.
The abundant Higgs boson statistics which can be obtained at CLIC above 1 TeV, where the Higgs boson is produced predominantly through the WW-fusion process, improves the precision of the absolute couplings and also gives access to rarer processes, such as $t\bar{t}H$ and Higgs selfcoupling, which serve as indirect measurements of the top Yukawa coupling and the Higgs potential, respectively. Also, higher energy stages allow the measurement of rare Higgs decays like H$\rightarrow \gamma\gamma$ or H$\rightarrow \mu\mu$.
To exploit the results obtained independently at each energy stage, the simultaneous fit of the full data sample is performed. In a model-independent fit, the majority of the accessible couplings are measured at the percent level. Using the fit which constraines the total Higgs decays width to the SM expectations, model-dependent fit, the result is improved to the sub-percent level.

References

[1] G. Aad et al., *Observation of a new particle in the search for the Standard Model Higgs boson with the ATLAS detector at the LHC*, Phys.Lett. **B716** (2012) 1, DOI: 10.1016/j.physletb.2012.08.020, arXiv:1207.7214 [hep-ex].

[2] S. Chatrchyan et al., *Observation of a new boson at a mass of 125 GeV with the CMS experiment at the LHC*,

Phys.Lett. **B716** (2012) 30, DOI: 10.1016/j.physletb.2012.08.021, arXiv:1207.7235 [hep-ex].

[3] M. S. L. Linssen A. Miyamoto, H. Weerts, eds., *CLIC Conceptual Design Report: Physics and Detectors at CLIC*, CERN-2012-003, CERN, 2012, arXiv:1202.5940 [physics.ins-det].

[4] M. P. S. Lukić I. Božovic-Jelisavčić, I. Smiljanić, *Correction of beam-beam effects in luminosity measurement in the forward region at CLIC*, JINST **8** (2013) P05008, arXiv:1301.1449 [hep-ex].

[5] M. Venturini, W. Kozanecki, *The hourgalss effect and the measurement of the transferse size of colliding beams by luminosity scans*, Proceedings IEEE Particle Accelerator Conference (2001) 3573.

[6] T. Abe et al., *The International Large Detector: Letter of Intent* (2010), arXiv:1006.3396 [hep-ex].

[7] M. O. E. H. Aihara (Ed.) P. Burrows (Ed.) et al., *SiD Letter of Intent* (2009), arXiv:0911.0006 [hep-ex].

[8] H. Abramowicz et al., *Physics at the CLIC e^+e^- - Linear Collider - Input to the Snowmass process 2013* (2013), arXiv:1307.5288 [hep-ex].

[9] C. Englert et al., *Precision Measurements of Higgs Couplings: Implications for New Physics Scales*, J. Phys. **G 41** (2014) 113001, arXiv:1403.7191 [hep-ph].

[10] M. A. Thomson, *Model-Independent Measurement of the e+e →HZ Cross Section at a Future e^+e^- Linear Collider using Hadronic Z Decays* (2015), arXiv:1509.02853 [hep-ex].

[11] E. S. C. Grefe, *Physics potential of the $\sigma(e^+e^- \to H\nu_e\bar{\nu}_e) \times BR(H \to Z\gamma)$ measurement at a 1.4 TeV Compact Linear Collider*, CLICdp-Note-2014-003 (2014).